will cancel the swing. Stopping anywhere between these points will result in residual oscillation.

The variation in oscillation amplitude with transport velocity for the "swing-free" trajectory is believed to be primarily due to small random oscillation of the shell before transport motion was begun. This violates the "zero initial conditions" constraint of the analysis. These random oscillations were caused by air currents from the building ventilating system.

Conclusions

A method has been shown for transporting suspended objects with a path-controlled robot manipulator such that the objects are stationary at the end of the motion. This method requires a manipulator capable of constant-velocity straight-line motion and an acceleration time that is small compared to the natural period of the suspended object. The method has been successfully used with a PUMA 600 manipulator to transport half-size wooden models of 8-inch artillery shells prior to inserting them into a perforated pallet.

Reference

1 Shames, I. H., *Engineering Mechanics*, Vol. II, *Dynamics*, Second Edition, Prentice-Hall, Inc., Englewood Cliffs, New Jersey, 1966.

Computer Simulation of Stick-Slip Friction in Mechanical Dynamic Systems

Dean Karnopp[1]

Stick-slip friction is present to some degree in almost all actuators and mechanisms and is often responsible for performance limitations. Simulation of stick-slip friction is difficult because of strongly nonlinear behavior in the vicinity of zero velocity. A straightforward method for representing and simulating friction effects is presented. True zero velocity sticking is represented without equation reformulation or the introduction of numerical stiffness problems.

1 Introduction

If a friction force F_f is plotted versus the relative velocity V between two contacting surfaces, a variety of relationships appear in practice. By stick-slip friction, we mean here a dry friction law such as that shown in Fig. 1(*a*) in which F_f at $V = 0$ can achieve a larger value than at moderate values of V.

Stick-slip friction often results in undesirable unstable dynamic behavior. The chattering of mechanisms and hunting of speed governors are often caused by stick-slip friction for example.

As Fig. 1(*a*) makes clear, it is difficult to linearize a dry friction law near $V = 0$. This means that linear dynamic models cannot be expected to predict effects such as chattering during slewing, sticking behavior at final positioning, or limit cycling around a final position which can be caused by stick-slip friction.

It is logical to use computer simulations to study the effects of stick-slip friction, but the representation of a friction law like that shown in Fig. 1(*a*) is not entirely straightforward. Neither of the causal input-output forms $F_f = F_f(V)$ or $V = V(F_f)$ is unique. Figure 1(*b*) shows a version of the friction law in which F_f is a unique function of V, but this law has physical and numerical problems.

Another approach involves switching input-output causalities. When the system "slips," $V \neq 0$ and $F_f = F_f(V)$. At $V = 0$, the system "sticks" and F_f takes on values determined by other elements of the system model. If F_f exceeds the breakaway force level, then the system switches back to the slip mode.

Here we show how to present true stick-slip behavior with constant causality and hence with a single set of state equations. Useful results are obtained without excessively short time steps.

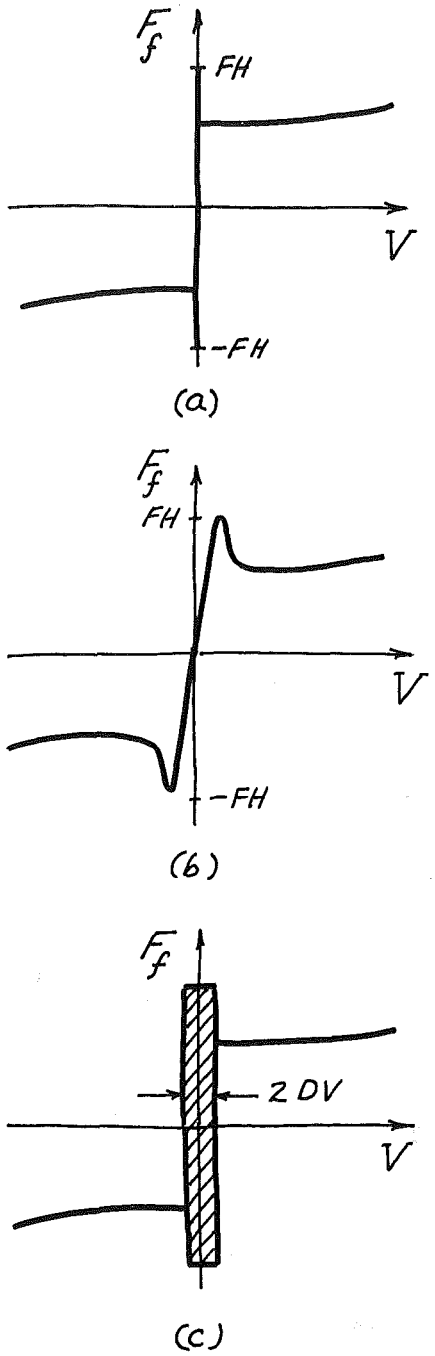

Fig. 1 Stick-slip friction laws

[1]Department of Mechanical Engineering, University of California, Davis, Calif. 95616.

Contributed by the Dynamic Systems and Control Division of THE AMERICAN SOCIETY OF MECHANICAL ENGINEERS. Manuscript received at ASME Headquarters, December 20, 1984.

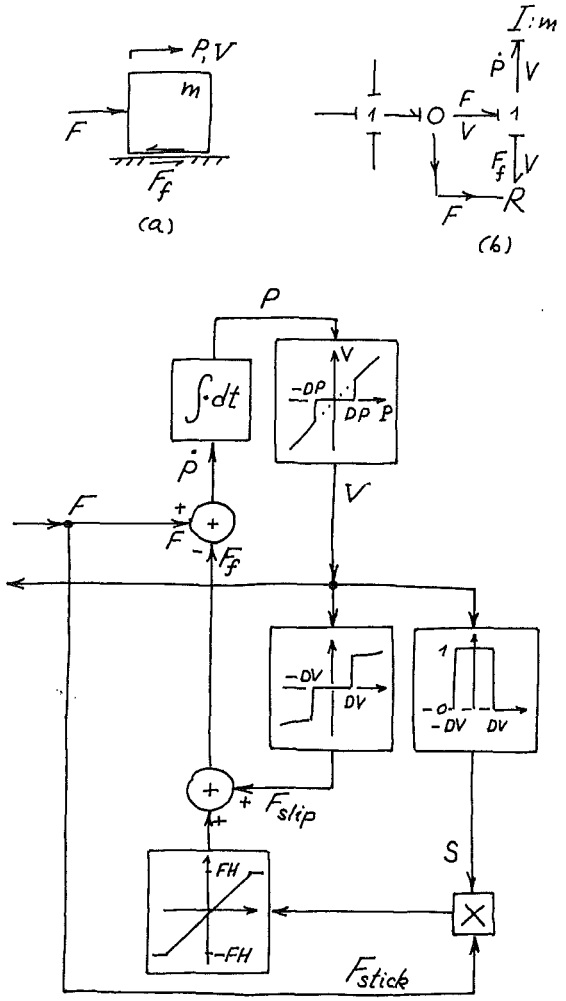

Fig. 2 Mass acted upon by a net force and friction

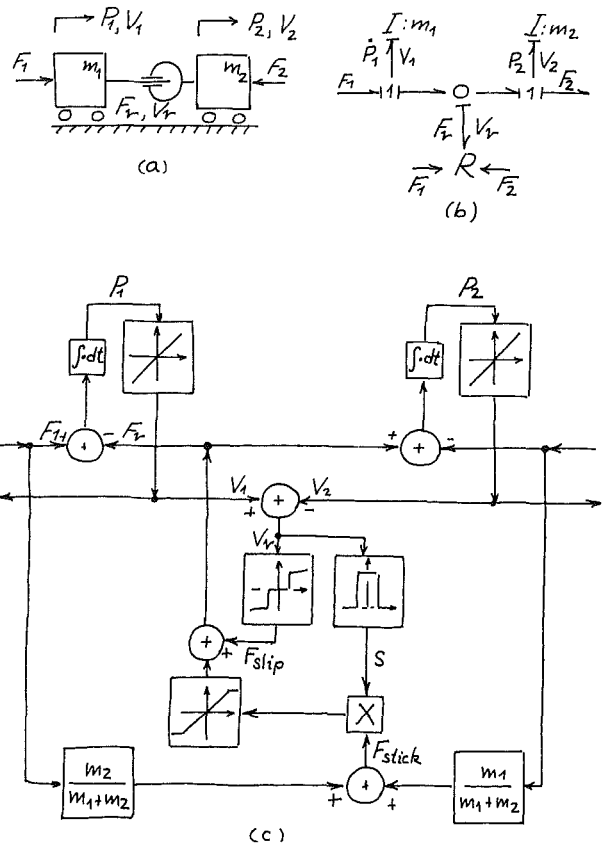

Fig. 3 Friction involving relative motion

II The Basic Model of Stick-Slip Friction

The friction law to be used is sketched in Fig. 1(*c*). In a sense, the friction force F_f is always a function of V. A region of small velocity is defined as $-DV < V < DV$. Outside this region, F_f is an arbitrary function of V. Inside the small region surrounding $V = 0$, we consider V to be zero. (The finite region is necessary for digital computation since an exact value of zero will not be computed.) Inside the $V = 0$ region, F_f is determined by other forces in the system in such a way that V remains in the region until the breakaway value of force is reached. The concept is best illustrated using the simple example of Fig. 2.

Consider the mass, m, with velocity V, momentum P, and friction force F_f. The force F is the net force on m from the rest of the system. The bond graph of part (*b*) shows the structure of the system (see reference [1]). Although the constant causality $F_f = F_f(V)$ is assumed, the active bond (or signal flow) shows that the force F also has an influence on the computation of F_f. The extra 2-port O-junction merely serves to define F as the active bond variable.

The block diagram of Fig. 2(*c*) corresponds to the bond graph of part (*b*). Note that F_f is composed of two parts. If $+DV < V < -DV$, then $F_f = F_{\text{slip}}$. The other component, a limited version of $S \cdot F_{\text{stick}}$ is zero in this case since the switch variable, S, vanishes in the slip region. On the other hand, in the stick region, $-DV < V < +DV$, $F_{slip} = 0$ and $S = 1$. So $F_f = F_{\text{stick}}$, but limited to the breakaway levels $\pm FH$.

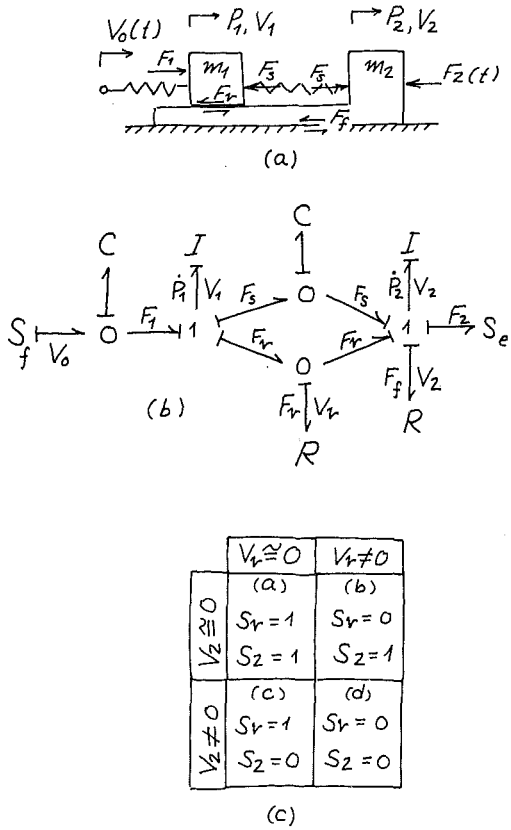

	$V_r \cong 0$	$V_r \neq 0$
$V_2 \cong 0$	(a) $S_r = 1$, $S_2 = 1$	(b) $S_r = 0$, $S_2 = 1$
$V_2 \neq 0$	(c) $S_r = 1$, $S_2 = 0$	(d) $S_r = 0$, $S_2 = 0$

(c)

Fig. 4 Complex example with interacting friction forces

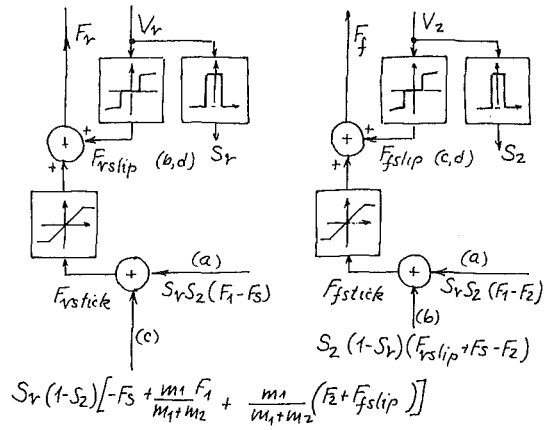

Fig. 5 Friction force generation for example of Fig. 4

The computation of the sticking force is very simple in this case. Newton's law for the mass is

$$\frac{dP}{dt} = F - F_f. \tag{1}$$

where P is the momentum, and thus the velocity V is

$$V = P/m. \tag{2}$$

In the sticking region, F_f takes on the force required to keep $V = 0$. This means $V = 0$ and $P = 0$, so

$$F_f = F_{\text{stick}} = F. \tag{3}$$

The limiter in the block diagram does not allow F_f to exceed the breakaway force level no matter what level F reaches. If $F > FH$, then F_f cannot counteract F, P, and V will no longer be zero, and the system will move into the slip region.

The upper part of the block diagram shows a useful trick. In the "stick" region, the momentum is constant and from equation (2), the velocity is also constant at some value between $\pm DV$. This means that when the mass is supposed to be sticking, it really has a small velocity. In many dynamic simulation studies, this small velocity does not affect the interpretation of the results, but it is easily possible to reduce the "sticking" velocity to zero by modifying the relation between V and P, equation (2), as shown in the block diagram of Fig. 2(*c*).

A momentum range is defined as

$$-DP < P < +DP \tag{4}$$

with

$$DP \equiv m \cdot DV \tag{5}$$

in which V is set to zero exactly. Thus, for finite values of DV and DP, the mass can remain at exactly zero velocity until the force moves P into the slip region after F_f has reached the breakaway force level. This concept allows true stick-slip motion to be achieved even with rather coarse adjustment of the switching boundary values DV and DP.

III Stick-Slip Friction Involving Relative Motion

Consider the case shown in Fig. 3 in which a friction element is inserted between two masses and reacts to the relative velocity V_r between them. As can be seen from either the bond graph or the block diagram, when $V_r \neq 0$, $F_r = F_{\text{slip}}$, and the system has two independent state variables P_1 and P_2.

However, if the system sticks at $V_r = 0$, then a knowledge of, say, P_1 and hence V_1 and the fact that $V_r = 0$ suffices to determine P_2 and V_2. We can consider P_1 and P_2 to be independent if we solve for the sticking force algebraically.

Assume the forces F_1 and F_2 are determined by system state variables. The state equations for m_1 and m_2 are

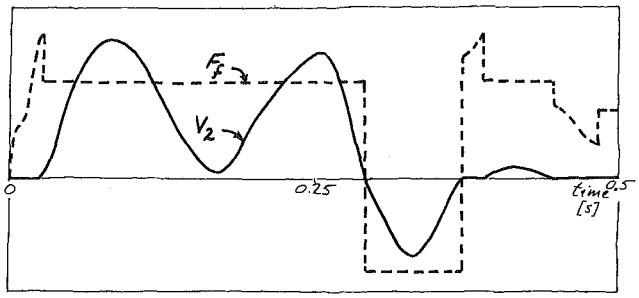

Fig. 6(*a*) F_f and V_2 versus time

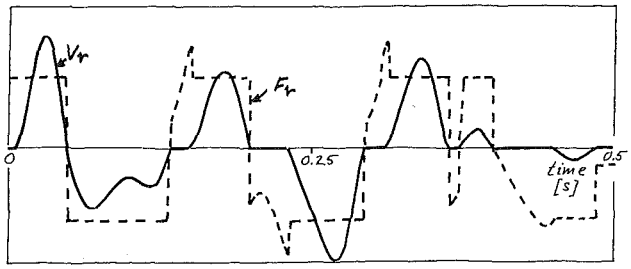

Fig. 6(*b*) F_r and V_r versus time

Fig. 6 Simulation results for example of Fig. 4

$$\dot{P}_1 = F_1 - F_r \tag{6}$$

$$\dot{P}_2 = F_2 - F_r \tag{7}$$

The velocities are

$$V_1 = P_1/m_1, \quad V_2 = P_2/m_2, \quad V_r = V_1 - V_2. \tag{8}$$

In the "sticking" region, $V_r = 0$ and F_r takes on the value F_{stick} required to keep V_r at zero. From equations (8), we find

$$\dot{V}_r = \dot{P}_1/m_1 - \dot{P}_2/m_2 \tag{9}$$

$$\dot{V}_r = (F_1 - F_r)/m_1 - (-F_2 + F_r)/m_2 \tag{10}$$

Then V_r will vanish when F_r takes the value

$$F_{\text{stick}} = \frac{m_2}{m_1+m_2} F_1 + \frac{m_1}{m_1+m_2} F_2 \tag{11}$$

In the block diagram of Fig. 3, F_r takes on either the value of F_{slip} or of F_{stick} limited by the breakaway force.

The forces F_1 and F_2 can be any forces which are not directly affected by the stick or slip state of the system. Such forces could be input forces, spring forces, or viscous friction forces. When several friction forces exist in a system and do not directly interact, they can be treated by the techniques shown in Figs. 2 and 3. On the other hand, when two or more stick-slip forces interact directly, the combination of stick-slip states must be considered. This is illustrated in the last example.

IV A More Complex Example

Figure 4 shows a case in which m_1 slides on m_2 which in turn slides on the ground. As the bond graph shows, the relative friction force F_r and the friction force F_f both act on m_2, so we cannot split the net forces up as in Figs. 2 and 3. We consider the four cases (*a*), (*b*), (*c*), and (*d*) in the logic diagram of Fig. 4(*c*) separately. The switching variables S_r and S_2 indicate whether both elements are sticking (*a*), slipping (*d*), or whether one is slipping and the other sticking (*b*), (*c*).

The block diagram fragments shown in Fig. 5 correspond closely to parts of Figs. 2 and 3. The only new feature involves the computation of the sticking forces $F_{r\text{stick}}$ and $F_{f\text{stick}}$ for F_r and F_f, respectively. The state equations for m_1 and m_2 are

$$\dot{P}_1 = F_1 - F_s - F_r, \tag{12}$$

$$\dot{P}_2 = F_s + F_r - F_f - F_2, \tag{13}$$

with

$$V_1 = P_1/m_1, \quad V_2 = P_2/m_2, \tag{14}$$

which can be read from the bond graph directly. The spring forces F_1 and F_s and the input force F_2 do not depend upon whether the friction elements stick or slip, but F_r and F_f take on different values, depending upon the conditions of V_r and V_2.

Consider first case (*a*) of Fig. 4(*c*). Both friction elements stick and we require V_r and V_2 to vanish. From equations (12), (13), and (14) we see that P_1 and P_2 also vanish and

$$F_{r\text{stick}} = F_1 - F_s, \tag{15}$$

$$F_{f\text{stick}} = F_1 - F_2. \tag{16}$$

In case (*b*), F_r is determined by $V_r \neq 0$,

$$F_r = F_{r\text{slip}} \tag{17}$$

but $\dot{V}_2 = 0$ which, using equations (13), (14), and (17), yields

$$F_{f\text{stick}} = F_s + F_{r\text{slip}} - F_2 \tag{18}$$

In case (*c*), F_f is determined by $V_2 \neq 0$,

$$F_f = F_{f\text{slip}}, \tag{19}$$

But $\dot{V}_r = 0$. Using equations (12), (13), and (14),

$$\begin{aligned}\dot{V}_r = \dot{V}_1 - \dot{V}_2 &= \dot{P}_1/m_1 - \dot{P}_2/m_2 \\ &= (F_1 - F_s - F_r)/m_1 \\ &\quad - (F_s - F_r - F_f - F_2)/m_2\end{aligned} \tag{20}$$

Then

$$F_{r\text{stick}} = -F_s + \frac{m_2}{m_1+m_2}F_1 + \frac{m_1}{m_1+m_2}(F_2 + F_{f\text{slip}}) \tag{21}$$

In case (*d*), both friction laws are in the slip regions so equations (17) and (19) apply.

The block diagram of Fig. 5 shows one way in which the forces F_r and F_f could be computed properly for all four cases. The switch variables S_r and S_2 only take on the values 0 or 1 so that the use of addition and multiplication allows the correct force computation.

Figure 6 shows the results of a simulation of the example system. The system equations for the bond graph of Fig. 4(*b*) were written automatically using the CAMP preprocessor, reference [3] but they could also have been written by hand using standard techniques. The friction force generation from Fig. 5 was then combined with the other system equations. The simulation was accomplished using CSMP III.

The plots of Fig. 6 show the response of the system starting at rest to a step in the input velocity V_0 which returned to zero at 0.25 s. The friction forces in the slip regions were constant and not a function of velocity (except for the sign). The breakaway force levels were 50 percent greater than the slip force levels.

The choice of DV for the two friction laws was not critical. As in Fig. 2, the P-V relationship was modified for both masses to yield zero velocity within the stick region. One can see just at the end of the plots that both masses come to rest. The printed values of velocity at rest are computed to be exactly zero. At several points in the plots, one can observe sticking with zero velocity, a subsequent rise of the friction force to its breakaway value, and then a drop to the slip value.

V Conclusions

The method for handling stick-slip friction is easily implemented for many practical actuator and mechanism problems. A modification of the inertia law relating velocity to momentum allows exact simulation of stopped motion.

The main advantage of this method of representing friction is that reasonable results are produced even when the limiting velocity DV is quite coarsely adjusted. This allows efficient simulation with relatively large time steps.

References

1 Rosenberg, R. C., and Karnopp, D. C., *Introduction to Physical System Dynamics*, McGraw-Hill, 1983.

2 Karnopp, D., and Rosenberg, R. C., *System Dynamics: A Unified Approach*, John Wiley and Sons, 1975.

3 Granda, J. J., *A Guide to Using CAMP* (Computer-Aided Modeling Program), Dept. of Mech. Eng., California State University, Sacramento, CA 95819.

A Generalized Solution to the Inverse Kinematics of Robotic Manipulators[1]

A. A. Goldenberg[2] and D. L. Lawrence[2]

In the context of kinematic control of a robotic manipulator if a certain set of task space coordinates (end effector position and orientation) are commanded then the corresponding configuration space coordinates (joint variables) must be provided. The joint variables are obtained by solving the "inverse kinematics problem." Typically a solution to the problem can be obtained in closed-form; however, such a solution is inherently manipulator-dependent. The paper presents an approach for providing a generalized inverse kinematics solution which is manipulator-independent. The solution is based on an iterative procedure. An algorithm was developed and demonstrated using the PUMA-560 and Stanford manipulator models.

1 Introduction

The inverse kinematics control of a robot manipulator requires the calculation of configuration space coordinates corresponding to a given set of task space coordinates. The common approach to this control problem is to use a closed-form solution to the inverse kinematic problem [1]. A major disadvantage of this approach is that closed-form solutions are manipulator-dependent. The method presented herein is based on an iterative solution to the inverse kinematics problem. Solutions are obtained with a moderate amount of computation.

The kinematic model used herein is obtained using the method developed by Denavit and Hartenberg [2]. The matrix equation defining the location (position and orientation) of the end effector in terms of the six joint variables is reduced to a system of six nonlinear equations. The solution is obtained by either least squares optimization or by a method treating the system as a set of simultaneous nonlinear equations. The solution converges rapidly (usually within fifty iterations) with arbitrary accuracy. The main advantage of this approach is that it may be applied to the inverse kinematics solution of *any* manipulator with six degrees of freedom for both simulation or real time control. A preliminary version of the work reported herein has been presented in [3].

The inverse kinematics problem of closed-loop kinematic

[1] The work was partially supported by NSERC Grant No. A-4664.

[2] University of Toronto, Department of Mechanical Engineering, Toronto, Ontario, Canada

Contributed by the Dynamic Systems and Control Division of THE AMERICAN SOCIETY OF MECHANICAL ENGINEERS. Manuscript received at ASME Headquarters, December 5, 1984.